(12) INTERNATIONAL APPLICATION PUBLISHED UNDER THE PATENT COOPERATION TREATY (PCT)

(19) World Intellectual Property Organization
International Bureau

(43) International Publication Date
14 June 2018 (14.06.2018)

WIPO | PCT

(10) International Publication Number
WO 2018/107142 A1

(51) International Patent Classification:
H01P 7/06 (2006.01) *G02F 1/355* (2006.01)
H01P 1/20 (2006.01) *G01N 21/3586* (2014.01)
H01P 5/02 (2006.01) *G01N 21/3581* (2014.01)
G02F 1/39 (2006.01) *H01Q 13/08* (2006.01)
G02F 1/35 (2006.01)

(21) International Application Number:
PCT/US2017/065524

(22) International Filing Date:
11 December 2017 (11.12.2017)

(25) Filing Language: English

(26) Publication Language: English

(30) Priority Data:
62/432,157 09 December 2016 (09.12.2016) US

(71) Applicants: **BROWN UNIVERSITY** [US/US]; Horace Mann Building, 47 George Street, 3rd Fl., Providence, Rhode Island 02912 (US). **OSAKA UNIVERSITY** [JP/JP]; 1-1 Yamadoaka, Suita-shi, Osaka, osaka 5650871 (JP).

(72) Inventors: **MENDIS, Rajind**; 92 Larch Street, Providence, Rhode Island 02906 (US). **NAGAI, Masaya**; 4-23-27-307, Miryayama-cho, Toyonaka, Osaka 5600056 (JP). **MITTLEMAN, Daniel M.**; 574 Angell Street, Providence, Rhode Island 02906 (US).

(74) Agent: **GUTERMAN, Sonia K.** et al.; Lawson & Weitzen LLP, 88 Black Falcon Ave., Suite 345, Boston, Massachusetts 02210 (US).

(81) Designated States *(unless otherwise indicated, for every kind of national protection available)*: AE, AG, AL, AM, AO, AT, AU, AZ, BA, BB, BG, BH, BN, BR, BW, BY, BZ,

(54) Title: POLARIZING BEAM SPLITTER FOR THZ RADIATION

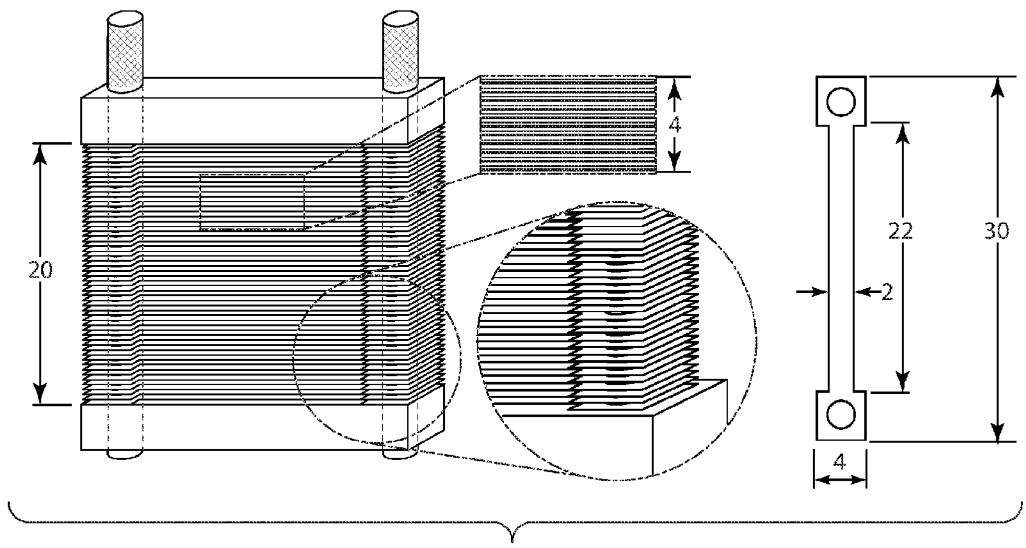

Figure 1A

(57) Abstract: A polarizing beam splitter includes thin electrically conductive metal sheets each having an edge and a thickness substantially less than the wavelength λ of a terahertz signal. The sheets are arranged in a stack or array to define wave propagation passages for energy of a terahertz beam directed at a face formed by edges of the sheets, and constitutes an artificial dielectric which operates below cutoff to allow selective transmission through the passages and/or reflection from said face, separating polarization states of the beam with defined power splitting. The artificial dielectric beam splitter can be configured to operate over a broad terahertz band. The sheets are flat, without micropatterned surface features, are robust and simple to manufacture, and form a broad band polarizing beam splitter for terahertz radiation. Complete separation of the transmitted and reflected beam is achieved below cutoff by rotating the polarization of the input beam.

WO 2018/107142 A1

[Continued on next page]

CA, CH, CL, CN, CO, CR, CU, CZ, DE, DJ, DK, DM, DO, DZ, EC, EE, EG, ES, FI, GB, GD, GE, GH, GM, GT, HN, HR, HU, ID, IL, IN, IR, IS, JO, JP, KE, KG, KH, KN, KP, KR, KW, KZ, LA, LC, LK, LR, LS, LU, LY, MA, MD, ME, MG, MK, MN, MW, MX, MY, MZ, NA, NG, NI, NO, NZ, OM, PA, PE, PG, PH, PL, PT, QA, RO, RS, RU, RW, SA, SC, SD, SE, SG, SK, SL, SM, ST, SV, SY, TH, TJ, TM, TN, TR, TT, TZ, UA, UG, US, UZ, VC, VN, ZA, ZM, ZW.

(84) **Designated States** *(unless otherwise indicated, for every kind of regional protection available)*: ARIPO (BW, GH, GM, KE, LR, LS, MW, MZ, NA, RW, SD, SL, ST, SZ, TZ, UG, ZM, ZW), Eurasian (AM, AZ, BY, KG, KZ, RU, TJ, TM), European (AL, AT, BE, BG, CH, CY, CZ, DE, DK, EE, ES, FI, FR, GB, GR, HR, HU, IE, IS, IT, LT, LU, LV, MC, MK, MT, NL, NO, PL, PT, RO, RS, SE, SI, SK, SM, TR), OAPI (BF, BJ, CF, CG, CI, CM, GA, GN, GQ, GW, KM, ML, MR, NE, SN, TD, TG).

Published:

— *with international search report (Art. 21(3))*

Polarizing Beam Splitter for THz Radiation

Government Support

This invention was made with government support under grant ECCS1609521 awarded by the National Science Foundation. The government has certain rights in the invention.

Background

Terahertz radiation, also known as submillimeter radiation, consists of electromagnetic waves within the band of frequencies from 0.1 to 10 terahertz (THz, where one THz is 10^{12} Hz). Wavelengths of radiation in the terahertz band correspondingly range from 3 mm to 0.03 mm (or 30 μm).

Terahertz radiation occupies a middle ground between microwaves and infrared light waves, and the technology or instrumentation for generation and manipulation of terahertz radiation is in its infancy. In the terahertz band or region of the electromagnetic spectrum, the frequency of electromagnetic radiation becomes too high to be measured digitally via electronic counters, so must be measured by proxy using the properties of wavelength and energy. Similarly, the generation and modulation of coherent electromagnetic signals in this frequency range ceases to be possible with the conventional electronic devices used to generate radio waves and microwaves, and thus will require development of new devices and techniques. However, generation, modulation and analysis of terahertz signals and their interactions also offer the prospect of new analytic measurements and detection utilizing characteristics and interactions that do not generally occur in nature. For example the *refractive index* of an artificial dielectric beam-shaping construction formed of stacked parallel plate waveguides, can have a value less than unity. Also, by way of example, photon energy in THz regime is less than band-gap of nonmetallic materials and thus THz beams can traverse through such materials. A transmitted THz beam can therefore be used for material characterization, layer inspection and developing transmission images. Although instrumentation for generating and for analyzing THz signals remains largely undeveloped, it is reasonable to expect that like lower frequency signals, THz radiation will, with appropriate instrumentation, be useful for communications and carry information signals, be analyzed to detect properties of material with which it has interacted, and serve as a probe for imaging and other measurement or detection purposes.

A polarizing beam splitter, if one could be devised for terahertz signals, would be highly useful for manipulating, separating, filtering, selectively blocking or conditioning terahertz radiation, and the development of such a beam splitter with robust and well-characterized performance characteristics would constitute an enabling event for further development of practical terahertz technologies and instruments.

There have been a few research studies on polarizing beam splitters for terahertz radiation, some based upon or analogous to the technology used for optical or microwave beam splitting - for example based upon dielectric bi-layers, or upon diffraction gratings, or metamaterial constructions. All of these attempts, however, called for advanced fabrication techniques requiring costly photolithography methods and equipment, and have limited prospects for mass production or general application to robust broadband applications.

There thus remains a need for a robust, well-characterized stable and easily manufactured polarizing beam splitter for terahertz signals that does not rely on micropatterned surface features.

Summary of the Invention

This is achieved in accordance with the present invention by providing an artificial dielectric medium formed as a uniformly-spaced stack or array of rectangular conductive metal plates each having an edge and being aligned with and spaced apart by a distance *d* from an adjacent plate, such that a portion of the beam directed at a virtual face defined by the plate edges is transmitted through the splitter by entering and travelling in the passage between plates to the opposite edge, and/or is partially reflected at the face. The reflected, or transmitted energy has defined magnitude and polarization state. For example, a linearly polarized terahertz radiation beam is split into two orthogonal polarization components in a pre-determined power ratio. The polarizing beam splitter so constructed can be used to separate illumination and return signals of an inspection instrument, or to accurately separate one polarization or a portion of a terahertz beam for separate processing or measurement. Importantly, by controlling the polarization of a terahertz signal directed at the beam splitter, the unit will operate below cutoff with low insertion loss and a defined splitting ratio.

In one representative prototype construction, the plates are smooth sheets of stainless steel 30 μm thick and are spaced 300 μm apart. The sheets are formed with a pair of throughholes positioned to fit over a pair of posts or rods which hold all sheets of the array in alignment, and each sheet is rectangular so that the stack forms a block with the set of sheet edges defining a virtual face of the block. The block may be mounted in a jig or fixture so that it may be positioned at an angle θ to the path of an incident beam, and oriented to directly transmit and reflect different polarizations along different paths, with a pre-determined power ratio. A metal other than stainless steel may be used to form the beamsplitter, so long as the metal is stiff enough to maintain the desired parallel-plate spacing and can be manufactured as a thin smooth sheet. The sheet thickness is small compared to the nominal wavelength λ of the terahertz signal, for example than $\lambda/10$, and the sheet spacing d is smaller than $\lambda/ 2\cos\theta$ to define narrow wave propagation passages between successive metal sheets to operate below cutoff. This stacked parallel plate waveguide (PPWG) assembly configured as a polarization beam splitter can be fabricated without specialized surface patterning, and operates over a broad band with well defined splitting ratio and low insertion loss.

By way of background, an artificial dielectric lens construction using parallel plate waveguides has been previously described in *Scient. Rep.* **6**, 23023 (2016) using a stack of plates with a plano-concave shape that results in convergent beam focusing to a 4 mm spot at a design frequency of 0.17 THz. During that investigation, it was noted that the overall power transmission of the artificial dielectric lens can be better than that of conventional dielectric lenses commonly used in the THz regime; and further that under certain conditions the lens boundary demarcated by the plate edges actually resembles a smooth continuous surface, but with a cutoff frequency dependent on the plate spacing. That investigation employed a 1 mm plate separation, corresponding to a refractive index of 0 at a cutoff frequency of 0.15 THz for propagation of the lowest-order transverse electric (TE_1) mode whose electric field vector is oriented parallel to the plates. Below cutoff, the TE_1 mode is totally reflected at the input face. Thus the beamsplitter allows the precise separation and transmission through the beamsplitter of the TEM mode. Moreover, by rotating the polarization of the input beam one can control or achieve a well-defined power division. Moreover, the transmitted TEM mode propagates between the plates without dispersion resulting in a well-defined time domain signal.

Brief description of the Drawings

These and other features of the invention will be understood from the Disclosure and the Claims appended hereto, taken together with the Figures wherein

Figure 1A shows (a) a perspective view of an artificial dielectric beamsplitter formed by a stack of conductive sheets (b) mounted on posts for insertion in a beam path;

Figure 1B shows FEM simulations at 0.2 THz of total transmission (left hand side) when the input is polarized perpendicular to the plates, and total reflection (right hand side) when the input is polarized parallel to the plates;

Figure 1C schematically illustrates beam reflection and beam transmission through the parallel plates below cutoff for electric fieldd polarized parallel and perpendicular to the plates.

Figure 2 shows the transmission spectra in the TE_1 mode, illustrating the cutoff when the input beam is at normal incidence to the device, and at 45° incidence (the standard operational configuration).

Figure 3 shows the reflection spectra in the TE_1 mode compared to a mirror (dark line). A figure inset shows the corresponding time-domain signals.

Figure 4 show the transmission spectra in the TEM mode compared to free-space (i.e., no device), where the inset shows the corresponding time-domain signals.

Figure 5 upper graph shows the Power Efficiency for the transmission (TEM) (lower trace) and the reflection (TE_1) (upper trace) arms, while the lower graph illustrates Extinction ratio for the transmission and reflection arms, respectively, measured with the input polarization at 45° to the plates.

Figures 6A and 6B illustrate fractional power division into the transmission and reflection arms as a function of the input polarization angle.

Detailed description

At the design frequency of 0.2 THz, our polarizing beam splitter (PBS) exhibits an extinction ratio of 42 dB in transmission and 28 dB in reflection with an overall insertion loss of 0.18 dB. These values rival the specifications of polarizing cube beamsplitters that are commercially available for visible and near-infrared wavelengths.

As described *supra,* the artificial dielectric medium consists of a uniformly spaced stack of identical, rectangular metal plates. This stack-of-plates is electromagnetically equivalent to a stacked array of parallel-plate waveguides (PPWGs). The plates are made of 30 μm thick stainless steel and are spaced 300 μm apart, as seen in the prototype device shown in Fig. 1(a). This aspect ratio of 1:10 between the plate thickness and the plate spacing was chosen to maximize device efficiency while at the same time, achieving mechanical robustness. Unnecessarily thick plates would result in undesirable reflection losses, while overly thin plates may not provide adequate robustness to realize the required uniform plate spacing. The plates and the spacers are fabricated by chemical etching to avoid introducing strain or creating burrs, and this helps to maintain plate flatness. The device is assembled by stacking the plates and spacers alternating along two locating posts, such that the plates are free-standing, supported only by their ends. At each end, there is an integrated square pad with a mounting hole. Once assembled, this stacked-plate arrangement results in a clear aperture of 20 mm. The magnified, close-up view of the 4 mm square section of the clear aperture illustrates the flatness of the plates and the uniformity of their spacing. Taking a slice across this image and using a graphical reconstruction method, we measured an average center-to-center plate spacing of 330 μm, with a standard deviation of 5 μm.

In the designed PBS device geometry, the THz beam is directed at the stack-of-plates at an angle of 45° to the virtual surface emulated by the plate edges, with the plane of incidence parallel to the plate surfaces. The operation of the PBS relies on both the TEM and TE_1 fundamental modes of the PPWG. When the input electric-field is linearly polarized perpendicular to the plates (*s*-polarized), only TEM modes are excited in the PPWG array, and the beam propagates through the device without altering its path. This behavior may be illustrated in a COMSOL FEM simulation result which plots the instantaneous electric field of the propagating beam along the axial cross-section parallel to the plate surfaces, at a frequency of 0.2 THz. As long as the input beam diameter is sufficiently larger than the plate spacing (for proper mode-matching) and the interaction path-length is short, this TEM-mode propagation will be a very efficient (i.e., low loss) process. On the other hand, when the input electric field is linearly polarized parallel to the plates (*p*-polarized), only TE_1 modes can be excited in the PPWG array, and the propagation is governed by the mode's cutoff frequency. Input frequencies that are above the cutoff will propagate through the device, while those that are below the cutoff will be reflected. In fact, these below-cutoff frequencies will be *totally* and *specularly* reflected in a well-defined beam, which may be illustrated in an FEM simulation result which plots the instantaneous magnetic field of the propagating beam at a frequency of 0.2 THz.

Under oblique incidence, the TE_1-mode cutoff frequency is given by $c/(2b\cos\alpha)$, where c is the free-space velocity, b is the plate spacing, and α is the incidence angle. For the demonstrated device, the cutoff is at 0.7 THz when the device is illuminated at 45°. Now, if the input electric-field is linearly polarized at an arbitrary angle (between 0° and 90°) to the plates, both the TEM and TE_1 modes are excited simultaneously. Then, the portion of the input beam (the perpendicular component) propagating via the TEM mode exits the device on axis, polarized perpendicular to the plates. This TEM-mode contribution is independent of the frequency. In contrast, the portion that could excite the TE_1 mode (the parallel component), if below cutoff, is totally reflected at 90° to the input axis, polarized parallel to the plates. By varying the angle of the input polarization, one can therefore control the power division into the two output arms, thereby realizing a versatile PBS. Incidentally, if there is any parallel component at a frequency above the cutoff, this portion would propagate through the device via the TE_1 mode and exit the device with a slight lateral shift, polarized parallel to the plates. The lateral shift is caused by the refraction of the beam inside the device due to the lower refractive index compared to free-space. Since the PBS operation would be somewhat degraded by any excitation of the TE_1 mode, the upper limit of the operational bandwidth of the PBS is set by the mode's cutoff frequency. It follows that the operational bandwidth can be increased by decreasing the plate spacing and/or increasing the incidence angle.

Experimental characterization

The prototype PBS device was experimentally investigated in both transmission and reflection configurations using a THz time-domain spectroscopy system. In this spectroscopy system, both the transmitter and receiver modules are fiber coupled to the main controller unit, so as to accommodate the multiple polarization axes and spatial configurations. Throughout the experiment, the device was located between two wire-grid polarizers to purify the input and detected linear polarizations. Via external optics, the input beam was formed to a frequency-independent $1/e$ Gaussian diameter of approximately 10 mm and entered the device fairly well collimated. The same optical arrangement was employed for the output beam to maintain input-output symmetry. While the input optics were fixed in space, the detector sub-system could be moved (intact) from the on-axis position to the 90°-off-axis position to change from a transmission configuration to a reflection configuration. A 16 mm diameter aperture was situated in close proximity to the input transverse-plane of the device. This eliminated any energy "spill-over", providing a true reference signal when the device was not in the beam path, and also served as a marker for the beam axis. In addition to three-axis linear translation, the device mount also included a precision rotation stage to adjust the incidence angle in the horizontal plane, along with precision control of the tilt in two perpendicular vertical planes, allowing complete three-axis rotational positioning.

Various measured amplitude spectra that were obtained by Fourier transforming the detected time-domain signals are shown in Fig. 2. These spectra correspond to the purely TE_1-mode behavior of the device in transmission. During this measurement, both the transmitter and receiver polarization axes (along with the input and output polarizer axes) were kept horizontal. One curve corresponds to the reference signal when there is no device in the path of the beam. The sharp dips seen at 0.56 THz and 0.75 THz are due to water vapor absorption. Another curve corresponds to the signal when the device is in the path of the beam at normal incidence. This spectrum indicates a cutoff near 0.5 THz, as expected for a 300 μm plate spacing. A further curve corresponds to the signal when the device is at 45° incidence (the designed operating configuration), and as predicted by theory, the cutoff shifts to a value near 0.7 THz. This TE_1-mode diagnostic measurement is indicative of the quality of the device and serves to estimate the operational bandwidth of the PBS.

For the spectra in Fig. 3, the polarization axes of the transmitter, receiver, and the polarizers were maintained horizontal as before, but the detector sub-system was moved to measure the reflected signal. One curve corresponds to the reflected signal when the device is at 45° incidence. Another curve corresponds to the reference signal when the device is replaced by a polished aluminum mirror. The detected time-domain signals, along with the spectra, prove the highly efficient and non-dispersive broad-band operation of the device in reflection. The high-frequency attenuation of the device spectrum which appears to build up starting close to 0.7 THz is consistent with the TE_1-mode transmission spectrum in Fig. 2. Since this attenuation manifests for relatively low amplitude levels of the input spectrum (as evident by the reference), there is only minimal change in the reflected temporal signal.

To obtain the spectra in Fig 4, the measurement configuration was changed back to transmission, and the polarization axes of the transmitter, receiver, and the polarizers, were rotated to be vertical, a configuration to investigate the purely TEM-mode behavior of the device. One curve corresponds to the reference signal when there is no device in the beam path. Another curve corresponds to the signal when the device is at 45° incidence to the input beam. Detected time-domain signals, along with the amplitude spectra, proved the highly efficient and non-dispersive broad-band operation of the device in transmission. This observation is not surprising since the TEM mode of the PPWG is a very low-loss and dispersion-less propagating mode. However, it should be noted that in order to obtain this efficient propagation it was important for the collimated beam axis to be aligned so as to be parallel to the plate surfaces with high accuracy, and also for the input polarization direction to be exceptionally well perpendicular to the plate surfaces. Deviations from these two conditions (by more than a few degrees) would result in additional losses, as the oblique incidence results in a longer interaction path-length, compared to that with normal incidence. It is not only the added ohmic loss that comes into play here, but also the relative parallelism of the stack of plates.

Using the above spectra, we can deduce the power efficiency of the device for the transmission and reflection arms. These efficiency curves are plotted in Figure 5(a) for transmission and reflection, respectively, within the operational bandwidth of the PBS. For the reflection arm, the efficiency curve is relatively flat throughout the bandwidth, and indicates a power efficiency of 96% at both 0.2 THz and 0.5 THz, for example. This corresponds to an insertion loss of only 0.18 dB. For the transmission arm, the efficiency is 96% at 0.2 THz, and drops to 84% at 0.5 THz. This corresponds to an insertion loss of 0.76 dB. For comparison, also plotted is the theoretical transmission (blue solid curve) taking into account only the ohmic loss associated with TEM-mode propagation. The discrepancy with the experimental curve (especially as the frequency increases) implies that there are other sources of loss. Part of this extra loss is caused by the non-negligible impedance mismatch at the input and output surfaces of the device, even in the case of TEM-mode propagation. This gives rise to two small reflections from these virtual surfaces, which may also be affected by the finite thickness of the plates. In fact, these reflections played a role in the subsequent measurements that were carried out to estimate the cross-polarization extinction ratios of the PBS.

In another measurement to estimate the extinction ratios, the input polarization was oriented at 45° to the horizontal plate surfaces, and both the vertical and horizontal components of the output were measured, for both the transmission and reflection configurations separately. Therefore, for the transmission arm, in addition to the major component of the output that is polarized perpendicular to the plates, this also measures the minor component that is polarized parallel to the plates. This minor cross-polarization component is a result of energy leakage due to subtle device imperfections. The squared ratio of these two components gives the extinction ratio as plotted in Fig 5(b), which indicates extinction ratios of 42 dB and 39 dB at 0.2 THz and 0.5 THz, respectively. Similarly, for the reflection arm, in addition to the major component polarized parallel to the plates, this measures the minor component polarized perpendicular to the plates. In this case, the cross-polarization component is due to the two TEM-mode reflections at the input and output surfaces, as discussed above. The estimated extinction ratio when plotted displayed some ripple is due to the associated Fabry-Perot effect, but showed extinction ratios of 28 dB and 22 dB at 0.2 THz and 0.5 THz, respectively. These values are not as impressive as for the transmission arm, but one way to improve this extinction would be to add a polarizer to the reflection arm.

The final characterization step of the PBS was to measure the power division into the two output arms as a function of the input polarization angle. Here, the input polarization is initially set parallel to the plate surfaces by the transmitter, and is rotated by the input-side polarizer in steps of 4°. Then, in the reflection configuration, the output is detected with the output-side polarizer (and receiver) oriented parallel to the plates. Similarly, in the transmission configuration, the output is detected with the output-side polarizer (and receiver) oriented perpendicular to the plates. The experimental results for the frequencies of 0.2 THz and 0.5 THz, are plotted in Figs. 6A and 6B, respectively, and agree very well with the theoretical power dependences of $\cos^4\theta$ and $\cos^2\theta\sin^2\theta$ given by the solid curves for the reflection and transmission arms, respectively. These results confirm that one can achieve a desired power division simply by rotating the input polarization axis, hence, a versatile PBS.

The foregoing description and report of the measurement results illustrates that the artificial dielectric polarizing beam splitter can be configured to operate with very high efficiency and high extinction ratios to separate polarization states of a terahertz beam, and that by initially rotating the input beam polarization one can achieve any desired power division, offering far better performance than other demonstrated methods. The conductive plate artificial dielectric construction is scalable to a range of terahertz frequencies.

These and other features of the invention will be understood from the description of exemplary embodiments above, and from the claims appended hereto.

What is claimed is:

1. A beam splitter or polarization filter for operation in connection with terahertz signals,

the splitter or filter comprising

a plurality of thin electrically conductive rectangular metal sheets each having an edge and a thickness less than a nominal wavelength λ of the terahertz signal and extending in a plane, the metal sheets being arranged in a stack or array parallel to each other at a spacing *d* smaller than $\lambda/2\cos\theta$ to define narrow wave propagation passages between successive metal sheets for terahertz energy of a beam directed at the stack at an angle θ,

wherein the stack or array constitutes an artificial dielectric such that when positioned in a path of a beam of terahertz radiation impinging on a face defined by said edges separates the beam into a first polarization component selectively transmitted along a transmission path in the passages between successive metal sheets and a second component reflected from said face, thus separating polarization states of the beam along different reflection and transmission paths.

2. A terahertz beamsplitter component comprising a stack of parallel conductive metal plates having a characteristic thickness and inter-plate spacing constituting an artificial dielectric and defining a plurality of narrow passages bound by respective pairs of the plates, the component being mounted and configured for transmission of radiation along said passages when the stack of plates is edgewise illuminated by an incident beam or signal of terahertz radiation below a cutoff frequency at an angle θ, and operative to totally reflect the incident beam below the cutoff frequency, selectively separating, transmitting or reflecting polarization states of the incident beam with defined power ratio over a broad terahertz band.

3. The component of claim 2, wherein the characteristic thickness of the plates is small compare to a nominal wavelength of the terahertz radiation such that a portion of beam energy enters and is transmitted through the narrow passages with a defined polarization state.

4. The component of claim 2, wherein the thickness of the plates is less than or about one tenth the spacing between plates and the plates are formed of stainless steel or a flat, stiff, smooth conductive metal.

5. The component of claim 2 or 4, wherein the plates are spaced apart by about $\lambda/2\cos\theta$ or less and are chemically etched to achieve uniform flatness without any burring of edges.

6. The component of claim 3, wherein beam energy is either transmitted through the passages or is totally specularly reflected as a well-defined beam, depending upon its frequency (or wavelength).

7. The component of claim 2 operative as a polarizing beam splitter or beam combiner.

8. A beam splitter or polarization filter for operation in connection with terahertz signals,

the splitter or filter comprising a stack of spaced-apart thin metal sheets having an aligned edge which, upon illumination by a terahertz beam at a defined angle of incidence θ transmits or reflects the beam and splits the polarization states of the beam.

9. The beam splitter of claim 8 positioned in a common transmission and receiving path of

an imaging or analysis instrument, or used in an information signal receiver, transmitter or processing instrument.

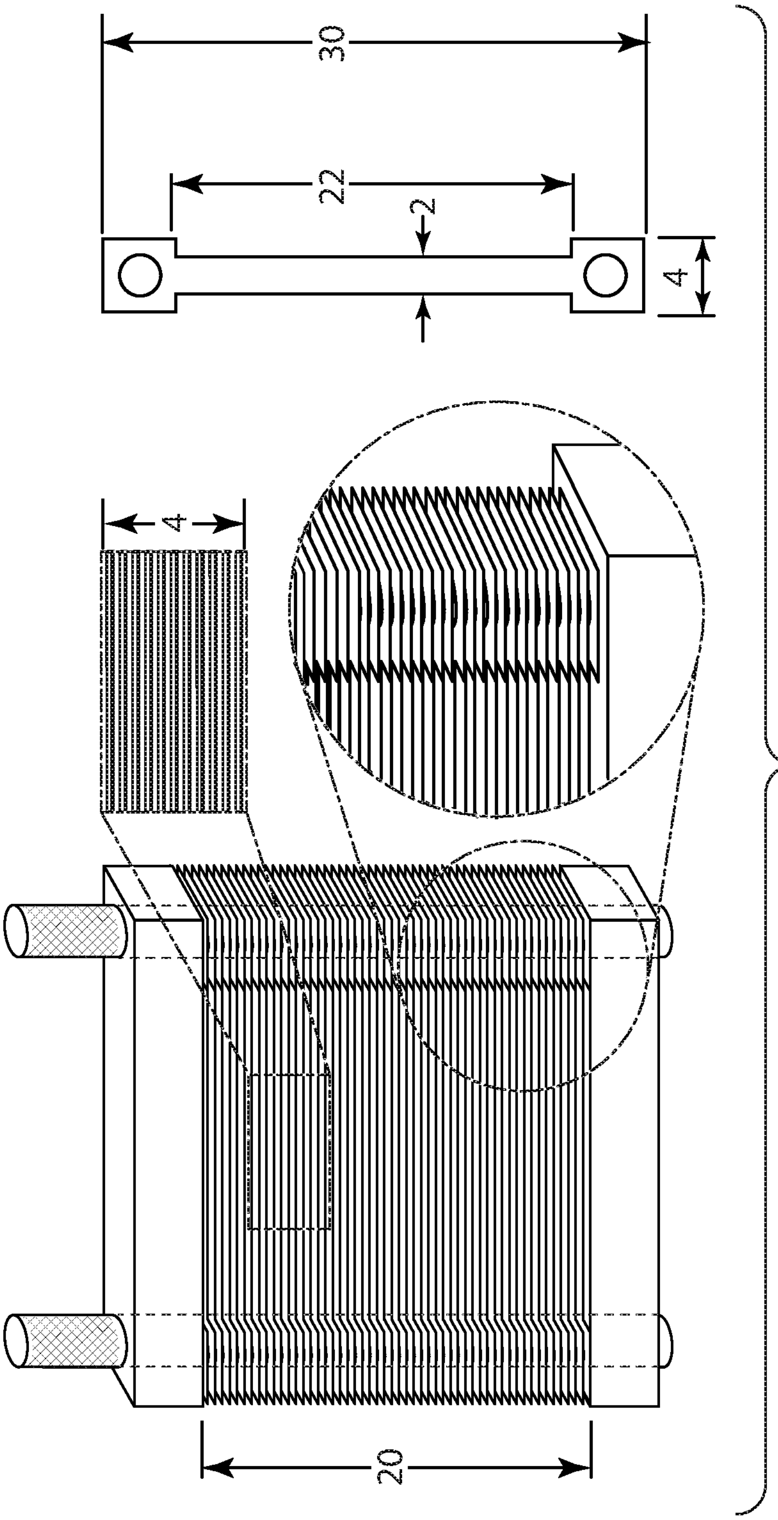

Figure 1A

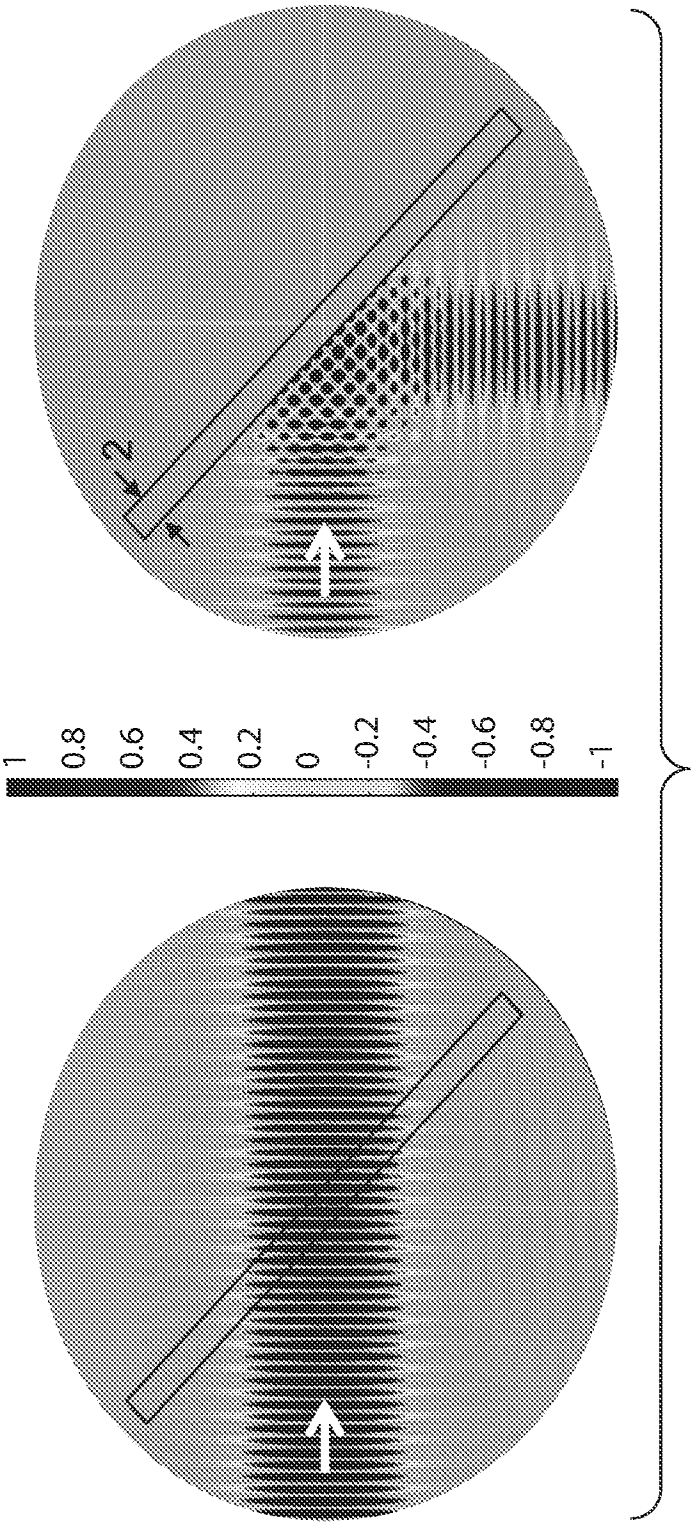

Figure 1B

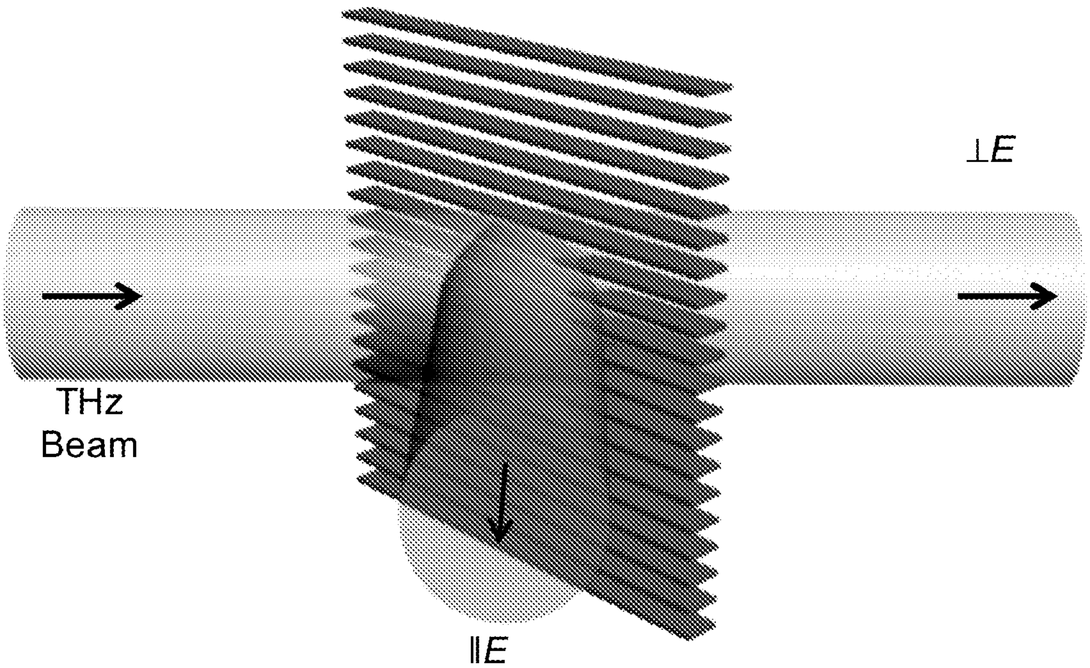

Figure 1C

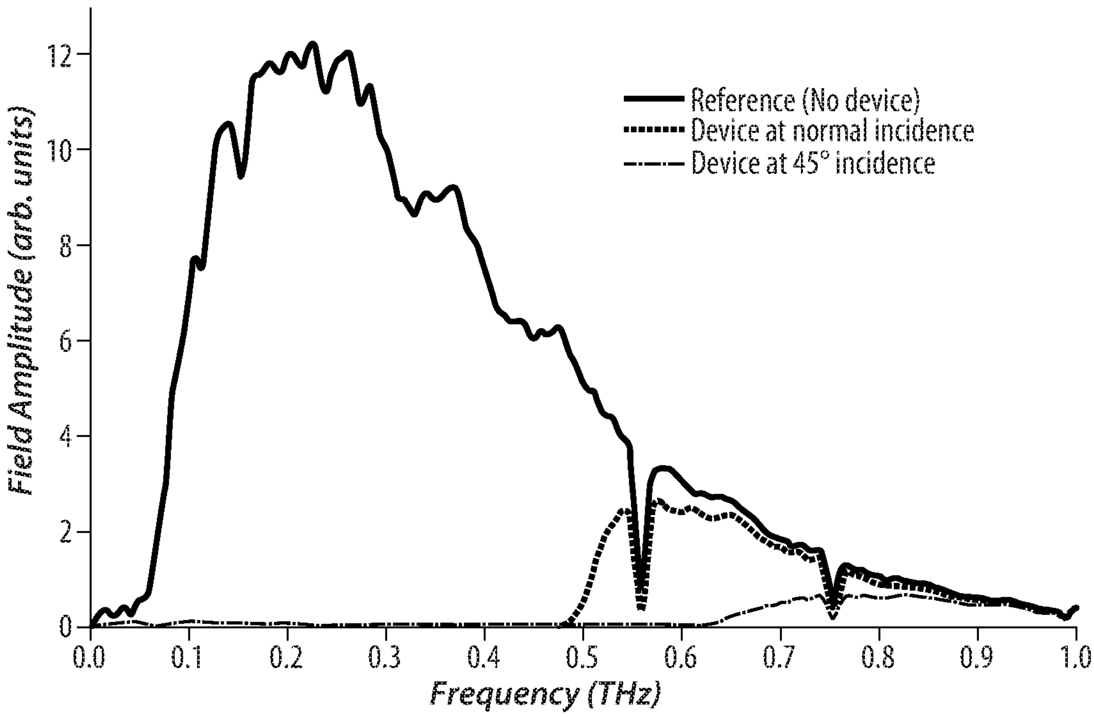

Figure 2

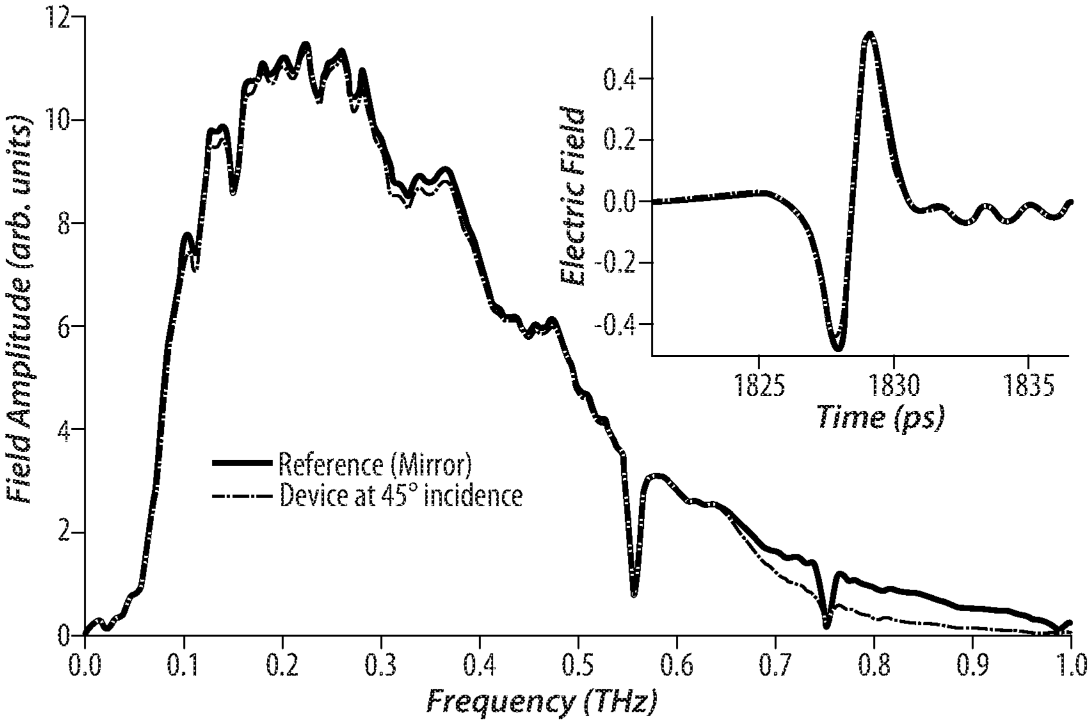

Figure 3

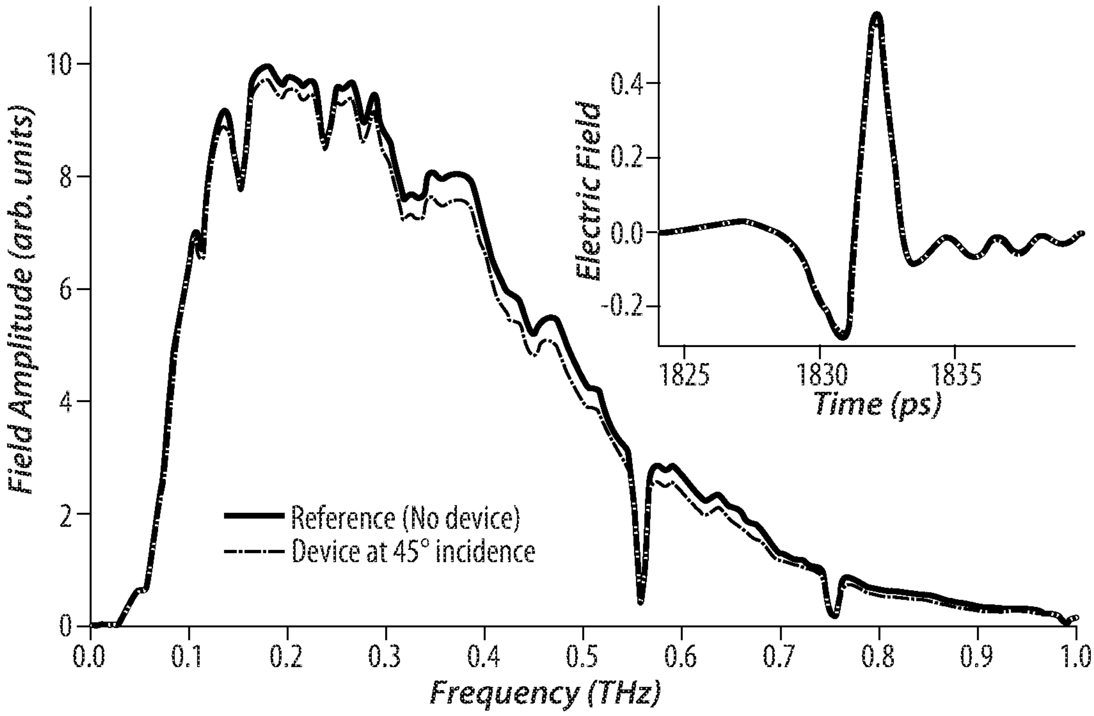

Figure 4

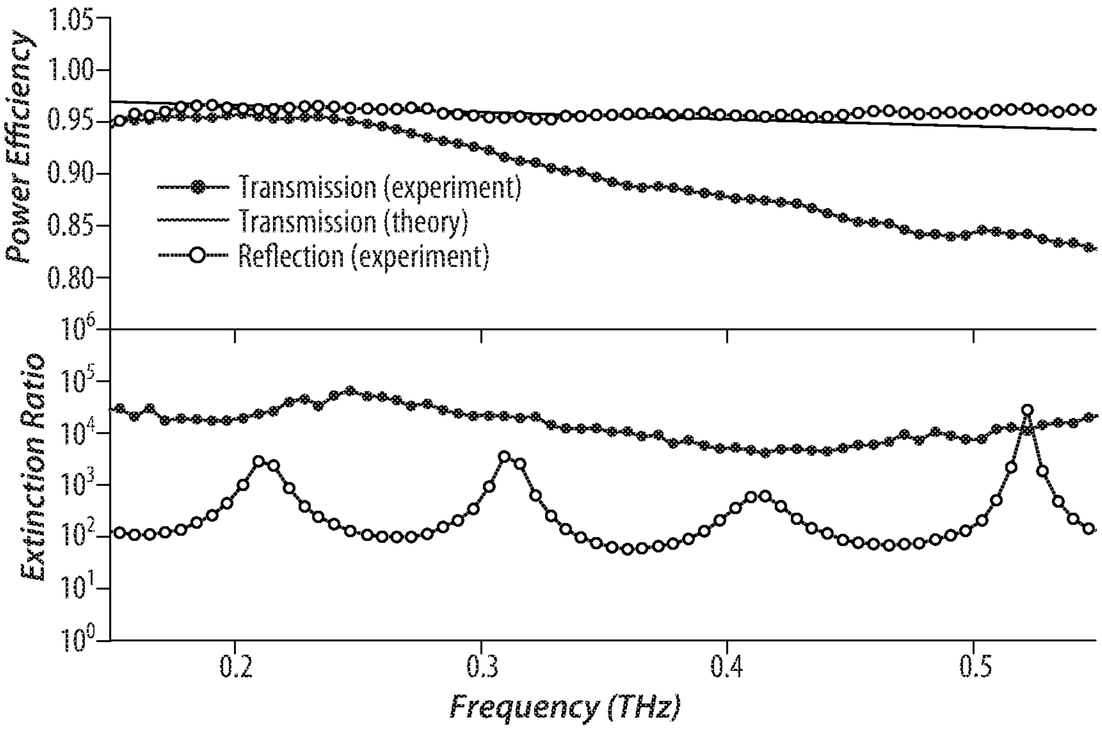

Figure 5

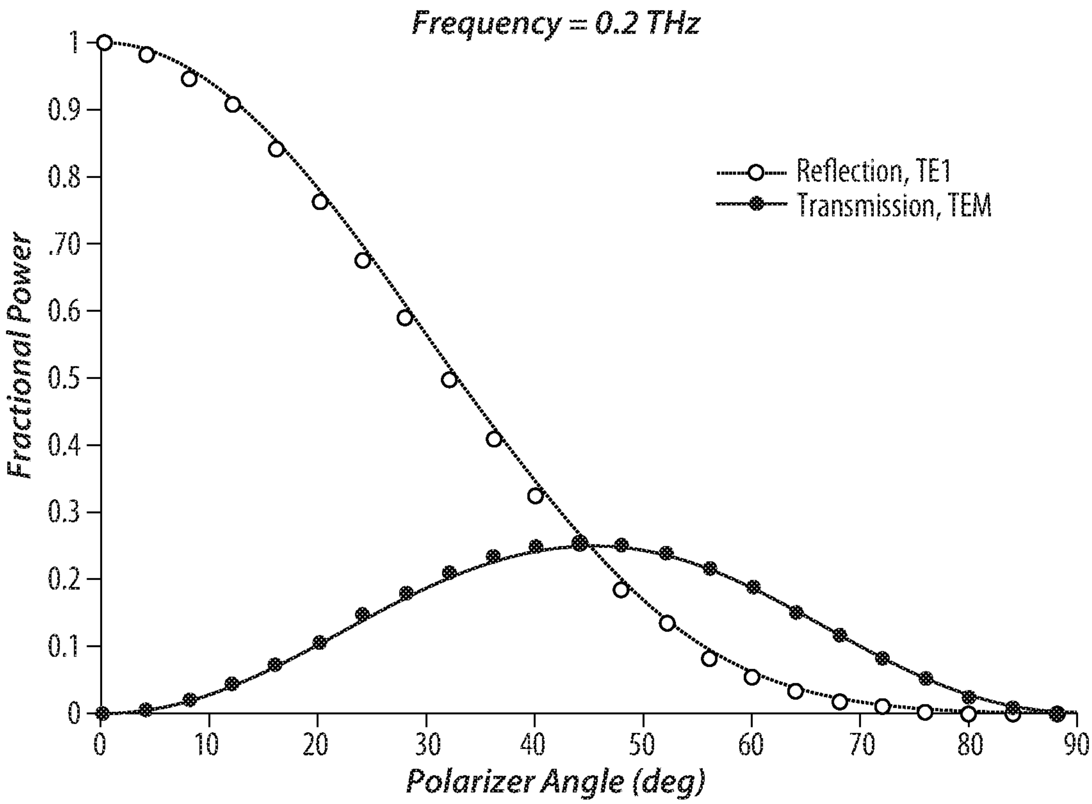

Figure 6A

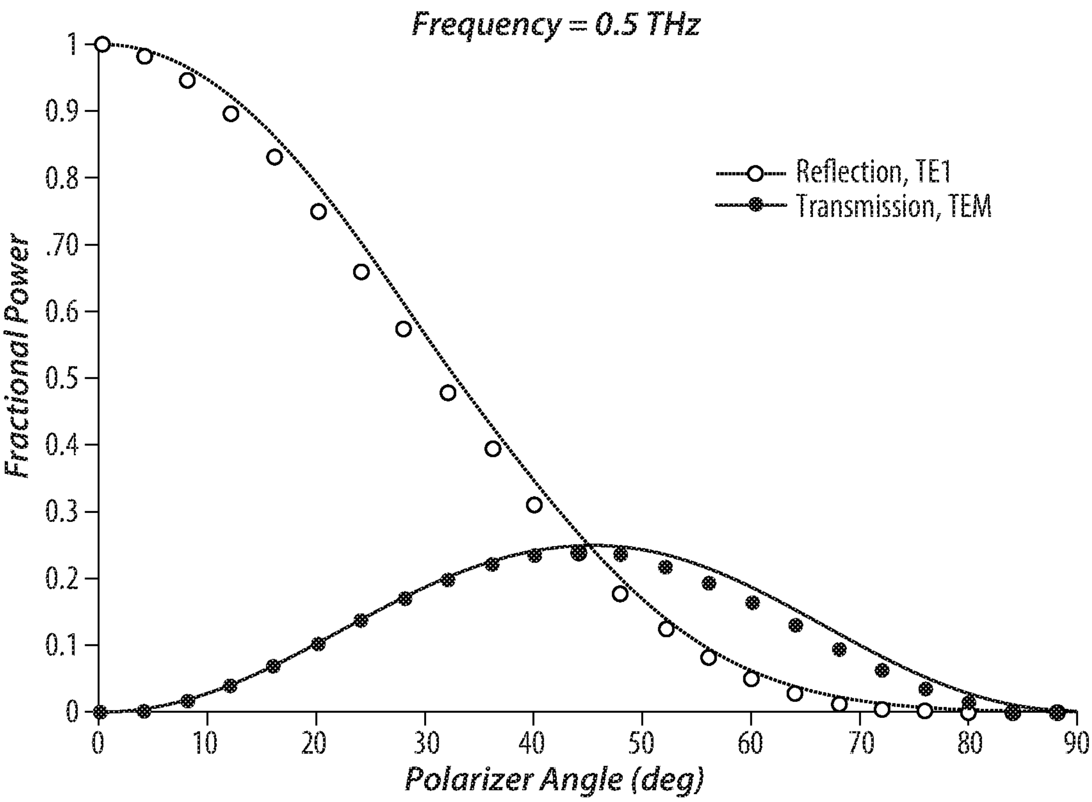

Figure 6B

INTERNATIONAL SEARCH REPORT

International application No.
PCT/US17/65524

A. CLASSIFICATION OF SUBJECT MATTER

IPC - H01P 7/06, 1/20, 5/02; G02F 1/39, 1/35, 1/355; G01N 21/3586, 21/3581; H01Q 13/08 (2018.01)

CPC - H01P7/06, 1/20, 5/02; G02F 1/39, 1/353, 1/3556; B82Y 20/00; G01N 21/3586, 21/3581; H01Q 13/08

According to International Patent Classification (IPC) or to both national classification and IPC

B. FIELDS SEARCHED

Minimum documentation searched (classification system followed by classification symbols)
See Search History document

Documentation searched other than minimum documentation to the extent that such documents are included in the fields searched
See Search History document

Electronic data base consulted during the international search (name of data base and, where practicable, search terms used)
See Search History document

C. DOCUMENTS CONSIDERED TO BE RELEVANT

Category*	Citation of document, with indication, where appropriate, of the relevant passages	Relevant to claim No.
X --- A	CN 105372758 A (UNIVERSITY JILIANG CHINA) March 2, 2016; see machine translation; abstract; paragraphs [0015], [0017]; claim 1	8-9 --- 1
A	CN 106058394 A (CHINA UNIVERSITY OF MINING) October 26, 2016; see maching translation; abstract; paragraphs [0025], [0036]; claim 1	1, 8-9
P, X	CN 106248616 A (SHENZHEN THZ INSTITUTE OF SCIENCE AND TECHNOLOGY INNOVATION) December 21, 2016; see machine translation	8, 9

☐ Further documents are listed in the continuation of Box C. ☐ See patent family annex.

* Special categories of cited documents:
- "A" document defining the general state of the art which is not considered to be of particular relevance
- "E" earlier application or patent but published on or after the international filing date
- "L" document which may throw doubts on priority claim(s) or which is cited to establish the publication date of another citation or other special reason (as specified)
- "O" document referring to an oral disclosure, use, exhibition or other means
- "P" document published prior to the international filing date but later than the priority date claimed
- "T" later document published after the international filing date or priority date and not in conflict with the application but cited to understand the principle or theory underlying the invention
- "X" document of particular relevance; the claimed invention cannot be considered novel or cannot be considered to involve an inventive step when the document is taken alone
- "Y" document of particular relevance; the claimed invention cannot be considered to involve an inventive step when the document is combined with one or more other such documents, such combination being obvious to a person skilled in the art
- "&" document member of the same patent family

Date of the actual completion of the international search	Date of mailing of the international search report
30 January 2018 (30.01.2018)	29 MAR 2018

Name and mailing address of the ISA/	Authorized officer
Mail Stop PCT, Attn: ISA/US, Commissioner for Patents P.O. Box 1450, Alexandria, Virginia 22313-1450 Facsimile No. 571-273-8300	Shane Thomas PCT Helpdesk: 571-272-4300 PCT OSP: 571-272-7774

Box No. II Observations where certain claims were found unsearchable (Continuation of item 2 of first sheet)

This international search report has not been established in respect of certain claims under Article 17(2)(a) for the following reasons:

1. ☐ Claims Nos.:
because they relate to subject matter not required to be searched by this Authority, namely:

2. ☐ Claims Nos.:
because they relate to parts of the international application that do not comply with the prescribed requirements to such an extent that no meaningful international search can be carried out, specifically:

3. ☐ Claims Nos.:
because they are dependent claims and are not drafted in accordance with the second and third sentences of Rule 6.4(a).

Box No. III Observations where unity of invention is lacking (Continuation of item 3 of first sheet)

This International Searching Authority found multiple inventions in this international application, as follows:
see extra sheet

1. ☐ As all required additional search fees were timely paid by the applicant, this international search report covers all searchable claims.

2. ☐ As all searchable claims could be searched without effort justifying additional fees, this Authority did not invite payment of additional fees.

3. ☐ As only some of the required additional search fees were timely paid by the applicant, this international search report covers only those claims for which fees were paid, specifically claims Nos.:

4. ☒ No required additional search fees were timely paid by the applicant. Consequently, this international search report is restricted to the invention first mentioned in the claims; it is covered by claims Nos.:
1, 8-9

Remark on Protest

☐ The additional search fees were accompanied by the applicant's protest and, where applicable, the payment of a protest fee.

☐ The additional search fees were accompanied by the applicant's protest but the applicable protest fee was not paid within the time limit specified in the invitation.

☐ No protest accompanied the payment of additional search fees.

-***-Continued from Box No. III Observations where unity of invention is lacking-***-

The application contains the following inventions or groups of inventions which are not so linked as to form a single general inventive concept under PCT Rule 13.1. In order for all inventions to be examined, the appropriate additional examination fee must be paid.

Group I: Claims 1, 8-9 are directed toward a beam splitter or polarization filter for operation in connection with terahertz signals.

Group II: Claims 2-9 are directed toward a terahertz beamsplitter component.

The inventions listed as Groups I and II do not relate to a single general inventive concept under PCT Rule 13.1 because, under PCT Rule 13.2, they lack the same or corresponding special technical features.

Group I has at least and a thickness less than a nominal wavelength 'A of the terahertz signal and extending in a plane, the metal sheets being arranged in a stack or array parallel to each other at a spacing d smaller than A/2cose that Group II does not have. Group II has at least the component being mounted and configured for transmission of radiation along said passages when the stack of plates is edgewise illuminated by an incident beam or signal of terahertz radiation below a cutoff frequency at an angle θ that Group I does not have.

The common technical features of Groups I-II are the splitter or filter comprising a stack of spaced-apart thin metal sheets having an aligned edge which, upon illumination by a terahertz beam at a defined angle of incidence θ transmits or reflects the beam and splits the polarization states of the beam. The common technical features are disclosed by CN105372758A to University of Jiliang China (hereinafter "Jiliang"). Jiliang discloses the splitter or filter comprising a stack of spaced-apart thin metal sheets having an aligned edge which (polarization beam splitter with stacked metal transmission layer and base metal layer; claim 1), upon illumination by a terahertz beam at a defined angle of incidence e transmits or reflects the beam and splits the polarization states of the beam (the terahertz wave illuminates the polarization beam splitter at an angle and outputs a beam at multiple polarization directions; paragraphs [0015], [0017]; claim 1).

Since the common technical features are previously disclosed by the Jiliang reference, these common features are not special and so Groups I-II lack unity.